UAV Relaying Assisted Secure Transmission With Caching

Fen Cheng, Guan Gui, *Senior Member, IEEE,* Nan Zhao, *Senior Member, IEEE,* Yunfei Chen, *Senior Member, IEEE,* Jie Tang, *Senior Member, IEEE,* and Hikmet Sari, *Fellow, IEEE*

***Abstract*—Unmanned aerial vehicle (UAV) can be utilized as a relay to connect nodes with long distance, which can achieve significant throughput gain owing to its mobility and line-of-sight (LoS) channel with ground nodes. However, such LoS channels make UAV transmission easy to eavesdrop. In this paper, we propose a novel scheme to guarantee the security of UAV-relayed wireless networks with caching via jointly optimizing the UAV trajectory and time scheduling. For every two users that have cached the required file for the other, the UAV broadcasts the files together to these two users and the eavesdropping can be disrupted. For the users without caching, we maximize their minimum average secrecy rate by jointly optimizing the trajectory and scheduling, with the secrecy rate of the caching users satisfied. The corresponding optimization problem is difficult to solve due to its non-convexity, and we propose an iterative algorithm via successive convex optimization to solve it approximatively. Furthermore, we also consider a benchmark scheme in which we maximize the minimum average secrecy rate among all users by jointly optimizing the UAV trajectory and time scheduling when no user has the caching ability. Simulation results are provided to show the effectiveness and efficiency of our proposed scheme.**

***Index Terms*—Caching, physical layer security, time scheduling, trajectory optimization, UAV relaying.**

I. Introduction

Unmanned aerial vehicles (UAVs) have been widely utilized in wireless networks to improve the system performance recently [1], which have many advantages. First, UAVs often provide line-of-sight (LoS) channel links with ground users, which can enhance the transmission performance significantly [2]. Then, UAVs can be deployed quickly and flexibly for on-demand wireless systems due to their high mobility and agility. In addition, UAVs are less expensive than traditional communication infrastructures such as ground base stations (BSs). Due to its promising performance, UAV assisted communication has attracted great interest from both industry and academia.

First, UAVs can be employed as aerial BSs to improve the capacity and coverage of traditional wireless networks [3]–[6]. For example, UAVs can be used to establish connections with users in some areas without infrastructures or achieve rapid service recovery after ground infrastructures being damaged in natural disasters. In [4], some fundamental work has been conducted to maximize the minimum throughput in multi-UAV networks via jointly optimizing the trajectory, power and scheduling. UAVs can also help ground BSs offload data traffic in crowded areas or improve the performance of cell-edge users [7]–[10]. Then, UAVs can be adopted as relays to help transmit information from source nodes to long-distance destination nodes [11]–[14]. Compared with ground static relays, UAV relay can achieve significant throughput gain because of its mobility and LoS channel. In [11], the throughput for UAV relaying system was maximized by designing UAV's trajectory and optimizing the source/relay transmit power. The outage probability of the UAV relaying network was significantly minimized by optimizing the UAV trajectory and power allocation in [12] and [13]. When there exist multi-layer UAV relays in the cellular network, mean packet transmission delay was minimized by optimizing resource allocation in [14]. In addition, UAVs should often connect to the core networks via limited wireless backhaul, which will degrade the user experience at peak-traffic hours. To overcome this problem, caching can be exploited for UAVs transmission to avoid network congestion [7], [15], [16]. In [15], the UAVs in a cloud radio access network were proposed to cache appropriate content during off-peak time via predicting users' behavior. An effective algorithm based on liquid state machine learning was proposed to predict the content request distribution of the users in LTE-U UAV networks [16]. In [7], the UAVs stored the enhancement layer segments of videos in advance, and then, they can fly close to the users who required the videos to provide transmission. Proactive caching can be also utilized to overcome the endurance issue for UAV communications, and some excellent work has been done in [17].

On the other hand, the security of wireless networks gains increasing attentions due to the broadcast characteristic of wireless channels [18], especially in UAV-assisted networks. This is because eavesdropper can intercept the information from the UAV more easily due to the LoS channel between the UAV and the eavesdropper. Recently, physical layer security is becoming an important technique to improve the network security via physical-layer methods [19]. Secrecy rate is a key metric to measure the performance of physical layer security, which denotes the rate of confidential information that can be

Manuscript received July 19, 2018; revised October 26, 2018 and December 20, 2018; accepted January 19, 2019. The work was supported by the National Natural Science Foundation of China (NSFC) under Grant 61871065, the open research fund of State Key Laboratory of Integrated Services Networks under Grant ISN19-02, the Fundamental Research Funds for the Central Universities under DUT17JC43, and the Xinghai Scholars Program. Part of this work has been published in preliminary form in the Proceedings of IEEE ICC 2019. The associate editor coordinating the review of this paper and approving it for publication was R. Zhang. *(Corresponding author: Nan Zhao.)*

F. Cheng and N. Zhao are with the School of Information and Communication Engineering, Dalian University of Technology, Dalian, Liaoning, P. R. China, and also with the State Key Laboratory of Integrated Services Networks, Xidian University, Xi'an, 710071, P. R. China (email: chengfen@mail.dlut.edu.cn, zhaonan@dlut.edu.cn).

G. Gui is with Nanjing University of Posts and Telecommunications, Nanjing, Jiangsu, China (e-mail: guiguan@njupt.edu.cn)

Y. Chen is with the School of Engineering, University of Warwick, Coventry CV4 7AL, U.K. (e-mail: Yunfei.Chen@warwick.ac.uk).

J. Tang is with the School of Electronic and Information Engineering, South China University of Technology, Guangzhou, Guangdong, P. R. China (Email: eejtang@scut.edu.cn).

H. Sari is with Nanjing University of Posts and Telecommunications, Nanjing, Jiangsu, China (e-mail: hikmet@njupt.edu.cn), and he is also the Chief Scientist of Sequans Communications, 92700 Colombes, France.

reliably transmitted without eavesdropping [20]. There have been plenty of works on physical layer security to disrupt the eavesdropping. The information beamforming and jamming beamforming were jointly optimized in [21] to guarantee the transmit and receive security for a full duplex BS. In [22], an overview of research on enhancing wireless transmission secrecy via cooperation was presented. The secure multiple amplify-and-forward relaying was studied in [23] over correlated fading channels. In [24], interference alignment was exploited to guarantee the secure transmission in wireless multi-user networks, and the methods of interference alignment and transceiver optimization for physical layer security were compared in [25]. In [26], artificial noise was generated and leveraged to improve the security of the cognitive non-orthogonal multiple access networks with simultaneous wireless information and power transfer. Two secure schemes of secure precoding were proposed for directional modulation systems via artificial noise in [27]. In [28], some fundamental research has been done to introduce artificial neural network to guarantee the security of cellular-connected UAVs. In [29], the joint trajectory design and user scheduling were applied in a novel dual-UAV-enabled wireless network to guarantee the secure transmission. Caching can be leveraged to improve the security of wireless networks, and in [30], the pre-cached file was transmitted along with the target file to cache-enabled user, which would disturb eavesdropping effectively.

Due to the LoS channel of UAV, the adversarial eavesdropping is a key threat for the UAV transmission, and some initial works have been focused on this aspect [31], [32]. In [31], the secrecy rate of UAV relaying systems was maximized by optimizing the transmit power of the source node and the UAV relay. In [32], the UAV trajectory was optimized to guarantee the secrecy rate from the UAV to the ground destination. Different from these works, in this paper, the secrecy rate of the UAV-relayed multi-user wireless network is guaranteed when there exists an eavesdropper, via using local caching and jointly optimizing the UAV trajectory and time scheduling.

The main motivations and contributions of this paper are summarized as follows.

- In this paper, the UAV trajectory and time scheduling are jointly optimized to guarantee the secure transmission in UAV-relaying systems with local caching. For every two users who have cached the file that is not required by themselves but required by the other, the UAV can broadcast the files cooperatively to them and disrupt the eavesdropping. For the users without caching, their secrecy rate should be improved through the trajectory optimization of UAV.
- In the optimization problem, the minimum secrecy rate of the uncached users is maximized through jointly maximizing the trajectory and time scheduling, with the secrecy rate requirement of caching users satisfied. The problem is a mixed-integer non-convex problem. We divide it into two subproblems, and propose an iterative algorithm to solve them alternately. The convergence of the algorithm is proved.
- We also consider the scenario in which no user is equipped with cache as a benchmark, and the minimum secrecy rate among all users is maximized through jointly optimizing UAV trajectory and time scheduling. The corresponding problem is also non-convex, which can be solved similarly as that with caching. Through comparison, we can conclude that local caching can help the UAV relaying assisted networks improve the security significantly.

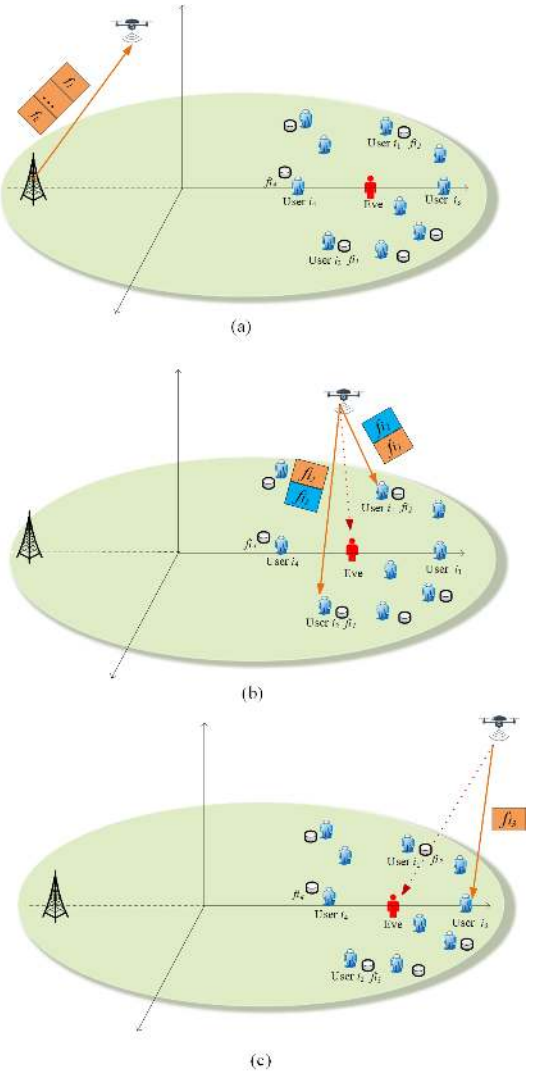

Fig. 1. UAV relaying assisted secure transmission with caching: (a) UAV obtains files from the BS; (b) UAV broadcasts files to User i_1 ($i_1 \in \mathcal{I}_1$) and User i_2 ($i_2 \in \mathcal{I}_2$); (c) UAV transmits file to User i_3 ($i_3 \in \mathcal{I}_3$).

The rest of the paper is organized as follows. We describe the system model and formulate the optimization problem in Section II. In Section III, an iterative algorithm is proposed to solve it through two subproblems alternately. In Section IV, the problem and its corresponding algorithm for the scenario without caching are presented. Simulation results are shown in Section V, followed by conclusions in Section VI.

II. System Model

A. System Model

We consider a UAV-enabled relaying communication system with one BS, multiple users and one eavesdropper on the

ground. The eavesdropper is close to the users. There are no direct links from the BS to the users and the eavesdropper due to long distance or blockages between them. The UAV is exploited as a mobile relay to ferry the information from the BS to the users owing to its mobility, as shown in Fig. 1(a). Assume that the users all require a specific file from a library denoted by $\mathcal{F}$, and the size of each file in the library is limited and proper due to the limited caching capacity of each user. In addition, assume that the UAV is equipped with a large-size cache, and the users have limited caching capacity. The users with caching capability can pre-cache some popular files during off-peak time. During the peak-traffic time, we assume that there are four different categories of users. Define $\mathcal{I}_l$ as the set of the users in the lth category, $l = 1, 2, 3, 4$. Assume that User i requires file i with data size W_i. The 1st category of users and the 2nd category of users have cached the files that are required by the users in the other category. For example, User i_1 in the 1st category ($i_1 \in \mathcal{I}_1$) has cached the file f_{i_2} required by User i_2 in the 2nd category ($i_2 \in \mathcal{I}_2$), and User i_2 in the 2nd category has cached the file f_{i_1} required by User i_1 in the 1st category. The UAV can broadcast f_{i_1} and f_{i_2} to them as shown in Fig. 1(b), which will disrupt the eavesdropping towards User i_1 or User i_2 via caching. The 3rd category of users have no caching abilities. When they obtain their required files from the UAV at different slots, they are much easier to be eavesdropped, as shown in Fig. 1(c). The users in the 4th category have cached their required files. Thus, they can obtain the required files directly from their local caches without eavesdropping. Meanwhile, it can help reduce the peak traffic and alleviate the backhaul load, which can avoid the network congestion. Thus, the secrecy rate of the users in the 3rd category should be guaranteed by optimizing the trajectory and time scheduling of UAV.

Without loss of generality, Cartesian coordinate is adopted to describe the proposed model. We assume that the horizontal locations of the BS, the eavesdropper and the ith user are denoted as $\mathbf{w}_b = (x_b, y_b)$, $\mathbf{w}_e = (x_e, y_e)$ and $\mathbf{w}_i = (x_i, y_i)$, respectively, $i \in \mathcal{I}_1 \cup \mathcal{I}_2 \cup \mathcal{I}_3 \cup \mathcal{I}_4$. The location of the ground eavesdropper can be detected and tracked by the UAV through the equipped optical camera or synthetic aperture radar [33], and thus the eavesdropping channel state information (CSI) can be obtained due to the LoS channel from UAV to the eavesdropper, which is a common assumption in the existing literature of UAV [31], [32]. The flight altitude and period of the UAV are assumed to be H and T, respectively. We can observe that a larger flight period T will achieve higher throughput since more time can be provided for the UAV to fly closer to each ground user to make better wireless channel. Nevertheless, larger T will also result in higher energy consumption and larger access delay since each user need to wait for longer time to communicate with the UAV in the next cycle. Therefore, we need to choose the period T properly to keep balance between the throughput, the access delay as well as the energy consumption. In addition, our proposed scheme can also be utilized in delay-tolerant applications and can exploit energy harvesting techniques such as solar energy to provide sufficient energy supply. The period T is divided into N equal time slots, i.e., $T = N\varsigma$, where ς is small enough to guarantee that the UAV's location is approximately unchanged within each slot. The horizontal position of the UAV at the nth time slot is denoted as $\mathbf{q}[n] = (x[n], y[n]), n = 1, 2, \ldots, N$. The UAV's maximum speed is assumed to be $V_{\max}$. Besides, we assume that the UAV's initial location is fixed, which is denoted as $\mathbf{q}_0 = (x_0, y_0)$. Thus, we have the trajectory constraints as

$$\begin{aligned} x[1] &= x[N] = x_0, \\ y[1] &= y[N] = y_0, \end{aligned} \tag{1}$$

$$\begin{aligned} (x[n+1] - x[n])^2 + (y[n+1] - y[n])^2 \le d_\varsigma^2, \\ n = 1, 2, \ldots, N-1, \end{aligned} \tag{2}$$

where $d_\varsigma = V_{\max} T/N$.

The UAV obtains the required files of the users from the BS first, and then transmits them to the users. Thus, the total N time slots are divided into two parts. Assume that the 1st slot to the N_1th slot are allocated to the UAV for obtaining the files required for the users from the BS[1], while the remaining slots are allocated to the UAV for transmitting the files to the users. The UAV cannot broadcast the files to cache-enabled users i_1 ($i_1 \in \mathcal{I}_1$) and i_2 ($i_2 \in \mathcal{I}_2$) and transmit file to user i_3 ($i_3 \in \mathcal{I}_3$) simultaneously due to interference. Instead, it serves the users without caching or cache-enabled user pairs via the time division multiple access (TDMA) protocol. For convenience, some binary variables, i.e., $\alpha_b[n]$ and $\alpha_i[n]$, $i \in \mathcal{I}_1 \cup \mathcal{I}_2 \cup \mathcal{I}_3 \cup \mathcal{I}_4$, are defined, which reflect the UAV time scheduling. The UAV obtains the files from the BS at the nth time slot if $\alpha_b[n] = 1$, otherwise, $\alpha_b[n] = 0$. Thus, we know that $\alpha_b[n] = 1, n = 1, ..., N_1$ and $\alpha_b[n] = 0, n = N_1 + 1, ..., N$. In addition, since User i_4 in the 4th category can obtain the desired file from its local cache, we have $\alpha_{i_4}[n] = 0$ over all slots. Furthermore, the UAV broadcasts f_{i_1} and f_{i_2} to User i_1 and User i_2 at the nth time slot if $\alpha_{i_1}[n] = \alpha_{i_2}[n] = 1$, otherwise, $\alpha_{i_1}[n] = \alpha_{i_2}[n] = 0$, $i_1 \in \mathcal{I}_1$, $i_2 \in \mathcal{I}_2$. Similarly, if $\alpha_{i_3}[n] = 1$, the UAV transmits f_{i_3} to User i_3 at the nth time slot, $i_3 \in \mathcal{I}_3$. Then, the following conditions should be satisfied as

$$\alpha_{i_1}[n] = \alpha_{i_2}[n] \in \{0, 1\}, \alpha_{i_3}[n] \in \{0, 1\}, \ \forall n, \tag{3}$$

$$\alpha_b[n] + \alpha_{i_1}[n] + \alpha_{i_3}[n] \le 1, \ \forall n, i_1 \in \mathcal{I}_1, i_2 \in \mathcal{I}_2, i_3 \in \mathcal{I}_3. \tag{4}$$

For simplicity, the wireless links from the BS to the UAV and from the UAV to the ground users and eavesdropper are assumed to be dominated by LoS. The Doppler effect due to the UAV mobility is assumed to be perfectly compensated at the receivers. Thus, the free-space path-loss model can be adopted, which is a common assumption in [4], [11], [31], [32]. Thus, when $\alpha_b[n] = 1$, the instantaneous rate in bit/second/Hz (bit/s/Hz) of the UAV at the nth time slot can be expressed as

$$r_{u,b}[n] = \log_2 \left(1 + \frac{P_1 \rho_0}{\sigma^2 \left(H^2 + (x[n] - x_b)^2 + (y[n] - y_b)^2\right)}\right), \tag{5}$$

where P_1 is the transmit power of the BS, σ^2 is the noise

[1]The UAV can first fly close to the users to collect the request information through uplink channel, and then inform the BS before relaying the files from BS to users via UAV in the upcoming cycle.

power, and ρ_0 is the reference channel power for the distance $d_0 = 1$ m.

Let z_{i_1} and z_{i_2} denote the signals of f_{i_1} and f_{i_2} with unit power, respectively. When $\alpha_{i_1}[n] = \alpha_{i_2}[n] = 1$, the UAV broadcasts the signal $\sqrt{\theta_{i_1} P_2} z_{i_1} + \sqrt{\theta_{i_2} P_2} z_{i_2}$ to User i_1 and User i_2 [30]. θ_{i_l} $(l = 1, 2)$ is the portion of the UAV's transmit power P_2 allocated to the file f_{i_l}, where $0 < \theta_{i_l} < 1$, $\theta_{i_1} + \theta_{i_2} = 1$. Since User i_l knows the pre-cached f_{i_j} perfectly, $j, l = 1, 2$, $j \neq l$, it can eliminate the interference f_{i_j} using the similar method of successive interference cancellation (SIC) in non-orthogonal multiple access (NOMA) [34]. Therefore, the instantaneous rate of User i_l $(l = 1, 2)$ at the nth time slot can be expressed as

$$r_{u,i_l}[n] = \log_2 \left(1 + \frac{\theta_{i_j} P_2 \rho_0}{\sigma^2 (H^2 + (x[n] - x_{i_l})^2 + (y[n] - y_{i_l})^2)}\right), \quad \forall l = 1, 2, i_l \in \mathcal{I}_l. \quad (6)$$

When $\alpha_{i_3}[n] = 1$, the instantaneous rate of User i_3 at the nth time slot can be expressed as

$$r_{u,i_3}[n] = \log_2 \left(1 + \frac{P_2 \rho_0}{\sigma^2 (H^2 + (x[n] - x_{i_3})^2 + (y[n] - y_{i_3})^2)}\right), \quad i_3 \in \mathcal{I}_3. \quad (7)$$

In addition, when the eavesdropper wants to eavesdrop User i_l, $l = 1, 2$, the instantaneous eavesdropping rate at the nth time slot can be expressed as

$$r_{u,ei_l}[n] = \log_2 \left(1 + \frac{\frac{\theta_{i_l} P_2 \rho_0}{H^2 + (x[n] - x_e)^2 + (y[n] - y_e)^2}}{\frac{\theta_{i_j} P_2 \rho_0}{(H^2 + (x[n] - x_e)^2 + (y[n] - y_e)^2)} + \sigma^2}\right), \quad \forall i_l \in \mathcal{I}_l, l, j = 1, 2, j \neq l, \quad (8)$$

where $\frac{\theta_{i_j} P_2 \rho_0}{(H^2 + (x[n] - x_e)^2 + (y[n] - y_e)^2)}$ is the interference from the file f_{i_j}. Since f_{i_j} is unknown by the eavesdropper, it will be viewed as interference to disrupt the eavesdropping when the eavesdropper aims to eavesdrop User i_l, $l = 1, 2$, $j \neq l$.

When the eavesdropper wants to intercept the information for User i_3, the instantaneous eavesdropping rate at the nth time slot can be presented as

$$r_{u,ei_3}[n] = \log_2 \left(1 + \frac{P_2 \rho_0}{\sigma^2 (H^2 + (x[n] - x_e)^2 + (y[n] - y_e)^2)}\right), \quad \forall i_3 \in \mathcal{I}_3. \quad (9)$$

Thus, the achievable average transmission rate for the UAV to obtain the files from the BS can be expressed as

$$R_u = \frac{1}{N} \sum\nolimits_{n=1}^{N} \alpha_b[n] r_{u,b}[n]. \quad (10)$$

The average transmission rate from the UAV to the ith user can be presented as

$$R^{[i]} = \frac{1}{N} \sum\nolimits_{n=1}^{N} \alpha_i[n] r_{u,i}[n], i \in \mathcal{I}_1 \cup \mathcal{I}_2 \cup \mathcal{I}_3. \quad (11)$$

The average secrecy rate from the UAV to the ith user can be denoted as

$$R_s^{[i]} = \frac{1}{N} \sum_{n=1}^{N} [\alpha_i[n] (r_{u,i}[n] - r_{u,ei}[n])]^+, i \in \mathcal{I}_1 \cup \mathcal{I}_2 \cup \mathcal{I}_3, \quad (12)$$

where $[x]^+ \triangleq \max(x, 0)$.

B. Problem Formulation

In this paper, we mainly aim at maximizing the minimum secrecy rate of the users without caching by jointly optimizing the UAV trajectory and time scheduling, with the secrecy rate of other caching users guaranteed. Define $\mathbf{A} = \{\alpha_k[n], \forall n, \forall k = b, i_1, ..., i_4, \forall i_l \in \mathcal{I}_l\}$, $\mathbf{x} = \{x[n], \forall n\}$, and $\mathbf{y} = \{y[n], \forall n\}$. The optimization problem can be formulated as

$$\begin{aligned}
(P1) \max_{\mathbf{A},\mathbf{x},\mathbf{y}} \quad & \phi_3 && (13a)\\
s.t. \ & R_s^{[i_3]} \geq \phi_3, \forall i_3 \in \mathcal{I}_3 && (13b)\\
& R_s^{[i_l]} \geq \eta, \ \forall i_l \in \mathcal{I}_l, l = 1, 2, && (13c)\\
& R^{[i_l]} \geq \beta^{[i_l]}, \forall i_l \in \mathcal{I}_l, l = 1, 2, 3, && (13d)\\
& R_u \geq \gamma, && (13e)\\
& \alpha_b[m] = 1, \ \forall m = 1, 2, ..., N_1, && (13f)\\
& \alpha_b[n] = 0, \ \forall n = N_1 + 1, ..., N, && (13g)\\
& \alpha_{i_1}[n] = \alpha_{i_2}[n] = \{0, 1\}, \alpha_{i_3}[n] = \{0, 1\}, \forall n, && (13h)\\
& \alpha_b[n] + \alpha_{i_1}[n] + \alpha_{i_3}[n] \leq 1, \ \forall n, && (13i)\\
& x[1] = x[N] = x_0, y[1] = y[N] = y_0, && (13j)\\
& (x[n+1] - x[n])^2 + (y[n+1] - y[n])^2 \leq d_\varsigma^2, \\
& n = 1, 2, \ldots, N - 1. && (13k)
\end{aligned}$$

Although the eavesdropping towards User i_1 and User i_2 can be effectively disrupted via local caching, to maximize the minimum secrecy rate of User i_3, more resource will be allocated to it, which will lead to a severe decline in the transmission rate of User i_1 and User i_2. Thus, to guarantee their performance, we add the secrecy rate constraints for these cached users as (13c), where η means the threshold of average secrecy rate for them. In addition, $\beta^{[i_l]}$ is the average transmission rate threshold of User i_l, which should satisfy $\beta^{[i_l]} \geq \frac{W_{i_l}}{BT}$. B is the channel bandwidth in Hertz. The constraint of the average transmission rate for the UAV to obtain the files from the BS is also added in (13e), where γ is its corresponding threshold satisfying $\gamma \geq \frac{\sum_{i_l \in \mathcal{I}_l} W_{i_l} + \sum_{i_2 \in \mathcal{I}_2} W_{i_2} + \sum_{i_3 \in \mathcal{I}_3} W_{i_3}}{BT}$.

It is important to notice that (P1) is non-convex due to the non-concave objective function and non-convex constrains. In addition, $R_s^{[i_l]}$ in (P1) is non-smooth at zero due to $[\cdot]^+$ in (12). Furthermore, (13f) to (13h) are integer constraints since the time scheduling variables are binary. Therefore, the optimization problem (P1) is quite difficult to solve directly, which will be further discussed in Section III.

III. Iterative Algorithm for Problem (P1)

In this section, we will propose an effective algorithm to solve the problem (P1) approximately. First, according to the following proposition, the objective function of (P1) can be changed to be smooth.

Proposition 1: The optimization problem (P1) can be expressed as the following problem $(\text{P1}')$ with the same

solutions.

$$(\mathrm{P1}^{'}) \max_{\mathbf{A},\mathbf{x},\mathbf{y}} \ \phi_3 \tag{14a}$$

$$s.t.\ \frac{1}{N}\sum_{n=1}^{N}\alpha_{i_3}[n]\left(r_{u,i_3}[n]-r_{u,ei_3}[n]\right)\geq\phi_3, \forall i_3\in\mathcal{I}_3, \tag{14b}$$

$$\frac{1}{N}\sum_{n=1}^{N}\alpha_{i_l}[n]\left(r_{u,i_l}[n]-r_{u,ei_l}[n]\right)\geq\eta, \forall i_l\in\mathcal{I}_l, l=1,2, \tag{14c}$$

$$\frac{1}{N}\sum_{n=1}^{N}\alpha_{i_l}[n]r_{u,i_l}[n]\geq\beta^{[i_l]}, \forall i_l\in\mathcal{I}_l, l=1,2,3, \tag{14d}$$

$$(13e)-(13k). \tag{14e}$$

Proof: It's obvious to find that the optimized secrecy rate of User i_3 at each time slot must be higher than or equal to 0, due to the fact that if the secrecy rate of User i_3 is less than 0 at the nth time slot, $\alpha_{i_3}[n]$ will be equal to 0 for maximizing the minimum average secrecy rate of the users without caching. In addition, the value of $r_{u,ei_l}[n]$ is always lower than or equal to that of $r_{u,i_l}[n]$ due to the interference from pre-cached file, $l=1,2$. Thus, the optimization problems (P1) and (P1$^{'}$) have same solutions. ■

According to Proposition 1, the problem (P1$^{'}$) has same solutions as those of (P1). Then, the integer constraints in (13h) are relaxed into continuous ones, and the optimization problem (P1$^{'}$) can be reformulated as

$$(\mathrm{P1}^{''}) \max_{\mathbf{A},\mathbf{x},\mathbf{y}} \ \phi_3 \tag{15a}$$

$$s.t.\ \frac{1}{N}\sum_{n=1}^{N}\alpha_{i_3}[n]\left(r_{u,i_3}[n]-r_{u,ei_3}[n]\right)\geq\phi_3, \forall i_3\in\mathcal{I}_3, \tag{15b}$$

$$0\leq\alpha_{i_1}[n]=\alpha_{i_2}[n]\leq 1, 0\leq\alpha_{i_3}[n]\leq 1, \forall n \tag{15c}$$

$$(14c), (14d), (13e), (13f), \tag{15d}$$

$$(13g), (13i), (13j), (13k). \tag{15e}$$

Although the above transformations have been performed, the optimization problem (P1$^{''}$) is still difficult to solve due to its non-convexity. Thus, (P1$^{''}$) is divided into two subproblems, which can be solved alternately through an iterative algorithm in next subsections.

A. Subproblem 1: Time Scheduling Optimization With Fixed Trajectory

The time scheduling optimization of (P1$^{''}$) can be expressed as the following subproblem with given trajectory.

$$(\mathrm{SP11}) \max_{\mathbf{A}} \ \phi_3 \tag{16a}$$

$$s.t.\ \frac{1}{N}\sum_{n=1}^{N}\alpha_{i_3}[n]\left(r_{u,i_3}[n]-r_{u,ei_3}[n]\right)\geq\phi_3, \tag{16b}$$

$$\frac{1}{N}\sum_{n=1}^{N}\alpha_{i_l}[n]\left(r_{u,i_l}[n]-r_{u,ei_l}[n]\right)\geq\eta, l=1,2, \tag{16c}$$

$$\frac{1}{N}\sum_{n=1}^{N}\alpha_{i_l}[n]r_{u,i_l}[n]\geq\beta^{[i_l]}, l=1,2,3, \tag{16d}$$

$$\frac{1}{N}\sum_{n=1}^{N}\alpha_{b}[n]r_{u,b}[n]\geq\gamma, \tag{16e}$$

$$\alpha_b[m]=1,\ \forall m=1,2,...,N_1, \tag{16f}$$

$$\alpha_b[n]=0,\ \forall n=N_1+1,...,N, \tag{16g}$$

$$\alpha_b[n]+\alpha_{i_1}[n]+\alpha_{i_3}[n]\leq 1,\ \forall n, \tag{16h}$$

$$0\leq\alpha_{i_1}[n]=\alpha_{i_2}[n]\leq 1, 0\leq\alpha_{i_3}[n]\leq 1, \forall n. \tag{16i}$$

It can be observed that (SP11) is a standard linear programming. Thus, we can solve it through using standard optimization tools such as CVX.

B. Subproblem 2: Trajectory Optimization With Fixed Time Scheduling

For any given time scheduling, the UAV trajectory optimization problem of (P1$^{''}$) can be expressed as

$$(\mathrm{SP12}) \max_{\mathbf{x},\mathbf{y}} \ \phi_3 \tag{17a}$$

$$s.t.\ \frac{1}{N}\sum_{n=1}^{N}\alpha_{i_3}[n]\left(r_{u,i_3}[n]-r_{u,ei_3}[n]\right)\geq\phi_3 \tag{17b}$$

$$\frac{1}{N}\sum_{n=1}^{N}\alpha_{i_l}[n]\left(r_{u,i_l}[n]-r_{u,ei_l}[n]\right)\geq\eta, l=1,2, \tag{17c}$$

$$\frac{1}{N}\sum_{n=1}^{N}\alpha_{i_l}[n]r_{u,i_l}[n]\geq\beta^{[i_j]}, l=1,2,3, \tag{17d}$$

$$\frac{1}{N}\sum_{n=1}^{N}\alpha_{b}[n]r_{u,b}[n]\geq\gamma, \tag{17e}$$

$$x[1]=x[N]=x_0, y[1]=y[N]=y_0, \tag{17f}$$

$$(x[n+1]-x[n])^2+(y[n+1]-y[n])^2\leq d_\varsigma^2, \quad n=1,2,\ldots,N-1. \tag{17g}$$

The problem (SP12) is difficult to solve due to the fact that the constraints in (17b), (17c), (17d) and (17e) are non-convex with respect to **x** and **y**. Thus, we transform (SP12) into a convex problem approximatively by utilizing successive convex optimization. Before the transformation, we introduce Lemma 1 as follows.

Lemma 1: Define a bivariate function as

$$f(\bar{x},\bar{y})=\log_2\left(1+\frac{D}{L+\bar{x}+\bar{y}}\right), \tag{18}$$

where $D>0$, $L>0$, $\bar{x}\geq 0$, and $\bar{y}\geq 0$. We have the

following inequality for any given $\bar{x}_0$ and $\bar{y}_0$.

$$\log_2\left(1+\frac{D}{L+\bar{x}+\bar{y}}\right)\geq\log_2\left(1+\frac{D}{L+\bar{x}_0+\bar{y}_0}\right)+\frac{-D\log_2 e}{(L+D+\bar{x}_0+\bar{y}_0)(L+\bar{x}_0+\bar{y}_0)}\left((\bar{x}-\bar{x}_0)+(\bar{y}-\bar{y}_0)\right). \tag{19}$$

Proof: The Hessian matrix of the function $f(\bar{x},\bar{y})$ can be expressed as

$$\nabla^2 f(\bar{x},\bar{y})=\begin{bmatrix} C & C \\ C & C \end{bmatrix}, \tag{20}$$

where

$$C=\frac{(2L+2\bar{x}+2\bar{y}+D)D\log_2 e}{\left((L+\bar{x}+\bar{y}+D)(L+\bar{x}+\bar{y})\right)^2}>0. \tag{21}$$

It can be concluded that the Hessian matrix is positive semidefinite when $\bar{x}\geq 0$, and $\bar{y}\geq 0$. Thus, the function is convex with respect to $\bar{x}$ and $\bar{y}$. Then, according to the fact that the value of the convex function is larger than or equal to that of its first-order Taylor expansion at any point [35], we obtain the inequation (19). ∎

$r_{u,k}[n],\forall k=b,i_1,i_2,i_3,\forall i_l\in\mathcal{I}_l$, in (17b), (17c), (17d), and (17e) is neither convex or concave with respect to $x[n]$ and $y[n]$. When we let

$$\bar{x}_k[n]=(x[n]-x_k)^2, \tag{22}$$

$$\bar{y}_k[n]=(y[n]-y_k)^2, \tag{23}$$

$r_{u,k}[n]$ is in the form of $\log_2\left(1+\frac{D_k}{L+\bar{x}_k[n]+\bar{y}_k[n]}\right)$, where $D_b=\frac{P_1\rho_0}{\sigma^2}$, $D_{i_l}=\frac{\theta_{i_l}P_2\rho_0}{\sigma^2}, l=1,2$, $D_{i_3}=\frac{P_2\rho_0}{\sigma^2}$ and $L=H^2$.

Then, according to Lemma 1, we can obtain

$$\begin{aligned} r_{u,k}[n]&\geq A_k^r[n]\left((\bar{x}_k[n]-\bar{x}_k^r[n])+(\bar{y}_k[n]-\bar{y}_k^r[n])\right)+B_k^r[n]\\ &=A_k^r[n]\big((x[n]-x_k)^2-\bar{x}_k^r[n]+(y[n]-y_k)^2-\bar{y}_k^r[n]\big)+B_k^r[n]\\ &\triangleq\check{r}_{u,k}[n],\ k=b,i_1,i_2,i_3,\forall i_l\in\mathcal{I}_l,\forall n, \end{aligned} \tag{24}$$

where $A_k^r[n]$, $B_k^r[n]$, $\bar{x}_k^r[n]$ and $\bar{y}_k^r[n]$ are the constants expressed as

$$A_k^r[n]=\frac{-D_k}{(L+D_k+\bar{x}_k^r[n]+\bar{y}_k^r[n])(L+\bar{x}_k^r[n]+\bar{y}_k^r[n])\ln 2}<0, \tag{25}$$

$$B_k^r[n]=\log_2\left(1+\frac{D_k}{L+\bar{x}_k^r[n]+\bar{y}_k^r[n]}\right), \tag{26}$$

$$\bar{x}_k^r[n]=(x^r[n]-x_k)^2, \tag{27}$$

$$\bar{y}_k^r[n]=(y^r[n]-y_k)^2, \tag{28}$$

where $\mathbf{x}^r=\{x^r[n],\forall n\}$ and $\mathbf{y}^r=\{y^r[n],\forall n\}$ describe the UAV flying trajectory in the rth iteration. It is observed that $\check{r}_{u,k}[n]$ is concave with respect to $x[n]$ and $y[n]$ since the value of $A_k^r[n]$ is less than 0. Then, for the secrecy rate of User i_3, we have

$$R_s^{[i_3]}\geq\frac{1}{N}\sum\nolimits_{n=1}^{N}a_{i_3}[n]\left(\check{r}_{u,i_3}[n]-r_{u,ei_3}[n]\right),\forall i_3\in\mathcal{I}_3. \tag{29}$$

In order to further transform the optimization problem into a convex one, the constraint in (17b) needs to be convex with respect to $x[n]$ and $y[n]$. Since $\check{r}_{u,i_3}[n]$ is concave with respect to $x[n]$ and $y[n]$, we can transform $r_{u,ei_3}[n]$ into a convex function to make the constraint in (17b) convex as follows.

We introduce slack variables as

$$\begin{aligned} \mathbf{S}=\big\{&S_{xe}[n]\mid S_{xe}[n]=(x[n]-x_e)^2,\\ &S_{ye}[n]\mid S_{ye}[n]=(y[n]-y_e)^2,\forall n\big\}. \end{aligned} \tag{30}$$

Then, $r_{u,ei_3}[n]$ expressed as (10) can be rewritten as

$$\begin{aligned} r_{u,ei_3}[n]&=\log_2\left(1+\frac{P_2\rho_0}{\sigma^2(H^2+S_{xe}[n]+S_{ye}[n]}\right)\\ &=\log_2\left(1+\frac{D_{i_3}}{\sigma^2(L+S_{xe}[n]+S_{ye}[n]}\right)\triangleq\hat{r}_{u,e}[n]. \end{aligned} \tag{31}$$

According to Lemma 1, $\hat{r}_{u,e}[n]$ is convex with respect to $S_{xe}[n]$ and $S_{ye}[n]$, which also makes $r_{u,ei_3}[n]$ convex. Thus, the constraint in (17b) can be approximatively transformed into convex.

On the other hand, the constraint (17c) can be approximately expressed as

$$\frac{1}{N}\sum\nolimits_{n=1}^{N}\alpha_{i_l}[n]\left(\check{r}_{u,i_l}[n]-r_{u,ei_l}[n]\right)\geq\eta,l=1,2. \tag{32}$$

Similarly, since $\check{r}_{u,i_l}[n]$ $(l=1,2)$ is concave, we can transform $r_{u,ei_l}[n]$ into a convex function to make the constraint (32) convex, $l=1,2$. For convenience, $r_{u,ei_l}[n]$ $(l=1,2)$ in (9) can be simplified as

$$\begin{aligned} r_{u,ei_l}[n]&=\log_2\left(1+\frac{P_2\rho_0}{\sigma^2\left(H^2+(x[n]-x_e)^2+(y[n]-y_e)^2\right)}\right)\\ &\quad-\log_2\left(1+\frac{\theta_{i_j}P_2\rho_0}{\sigma^2\left(H^2+(x[n]-x_e)^2+(y[n]-y_e)^2\right)}\right)\\ &=\hat{r}_{u,e}[n]-\log_2\left(1+\frac{\theta_{i_j}P_2\rho_0}{\sigma^2\left(H^2+\bar{x}_e[n]+\bar{y}_e[n]\right)}\right),\\ &\qquad\forall i_l\in\mathcal{I}_l,\forall l,j=1,2,j\neq l, \end{aligned} \tag{33}$$

where

$$\bar{x}_e[n]=(x[n]-x_e)^2, \tag{34}$$

$$\bar{y}_e[n]=(y[n]-y_e)^2. \tag{35}$$

Then, according to Lemma 1, we have

$$\begin{aligned} &\log_2\left(1+\frac{\theta_{i_j}P_2\rho_0}{\sigma^2\left(H^2+\bar{x}_e[n]+\bar{y}_e[n]\right)}\right)\\ &\geq E_{i_j}^r[n]\left((\bar{x}_e[n]-\bar{x}_e^r[n])+(\bar{y}_e[n]-\bar{y}_e^r[n])\right)+F_{i_j}^r[n]\\ &=E_{i_j}^r[n]\left((x[n]-x_e)^2-\bar{x}_e^r[n]+(y[n]-y_e)^2-\bar{y}_e^r[n]\right)+F_{i_j}^r[n]\\ &\triangleq\check{r}_{ei_l}[n],\ \forall i_l\in\mathcal{I}_l,\forall l,j=1,2,j\neq l, \end{aligned} \tag{36}$$

where $E_{i_j}^r[n]$, $F_{i_j}^r[n]$, $\bar{x}_e^r[n]$ and $\bar{y}_e^r[n]$ are the constants expressed as

$$E_{i_j}^r[n]=\frac{-D_{i_j}}{(L+D_{i_j}+\bar{x}_e^r[n]+\bar{y}_e^r[n])(L+\bar{x}_e^r[n]+\bar{y}_e^r[n])\ln 2}<0, \tag{37}$$

$$F_{i_j}^r[n]=\log_2\left(1+\frac{D_{i_j}}{L+\bar{x}_e^r[n]+\bar{y}_e^r[n]}\right), \tag{38}$$

$$\bar{x}_e^r[n]=(x^r[n]-x_e)^2, \tag{39}$$

$$\bar{y}_e^r[n] = (y^r[n] - y_e)^2. \tag{40}$$

Thus, $r_{u,ei_l}[n]$ in constraint (32) satisfies the following inequation.

$$r_{u,ei_l}[n] \leq \hat{r}_{u,e}[n] - \check{r}_{ei_l}[n], \ \ \forall i_l \in \mathcal{I}_l, \forall l = 1, 2. \tag{41}$$

Since $E_{i_j}^r[n] < 0$, $\check{r}_{ei_l}[n]$ is concave with respect to $x[n]$ and $y[n]$. In addition, $\hat{r}_{u,e}[n]$ is convex with respect to $S_{xe}[n]$ and $S_{ye}[n]$. Therefore, the constraint (32) can be transformed into convex as

$$\frac{1}{N}\sum\nolimits_{n=1}^{N} \alpha_{i_l}[n] \left(\check{r}_{u,i_l}[n] - \hat{r}_{u,e}[n] + \check{r}_{ei_l}[n]\right) \geq \eta, l = 1, 2. \tag{42}$$

Then, the optimization problem (SP12) can be rewritten as

$$\max_{\mathbf{x},\mathbf{y},\mathbf{S}} \ \phi_3 \tag{43a}$$

$$s.t. \ \frac{1}{N}\sum\nolimits_{n=1}^{N} \alpha_{i_3}[n] \left(\check{r}_{u,i_3}[n] - \log_2\left(1 + \frac{P_2\rho_0}{\sigma^2(H^2 + S_{xe}[n] + S_{ye}[n]}\right)\right) \geq \phi_3 \tag{43b}$$

$$\frac{1}{N}\sum_{n=1}^{N} \alpha_{i_l}[n] \left(\check{r}_{u,i_l}[n] - \hat{r}_{u,e}[n] + \check{r}_{ei_l}[n]\right) \geq \eta, l = 1, 2, \tag{43c}$$

$$\frac{1}{N}\sum_{n=1}^{N} \alpha_{i_l}[n]\check{r}_{u,i_l}[n] \geq \beta^{[i_j]}, l = 1, 2, 3, \tag{43d}$$

$$\frac{1}{N}\sum_{n=1}^{N} \alpha_b[n]\check{r}_{u,b}[n] \geq \gamma, \tag{43e}$$

$$S_{xe}[n] \leq (x[n] - x_e)^2, \forall n, \tag{43f}$$

$$S_{ye}[n] \leq (y[n] - y_e)^2, \forall n, \tag{43g}$$

$$(13j), (13k). \tag{43h}$$

It can be concluded that in (43f) and (43g), all constraints can be satisfied with equality to obtain the optimal solution, due to the fact that we can always increase $S_{xe}[n]$ and $S_{ye}[n]$ to enhance the objective value. However, the constraints in (43f) and (43g) are not convex with respect to $x[n]$ and $y[n]$. Thus, Lemma 2 is introduced to make the constraints in (43f) and (43g) convex.

Lemma 2: Define a quadratic function as

$$h(x) = (x - a)^2, \tag{44}$$

where a is a constant. For any given x^r, it satisfies the following inequality as

$$(x - a)^2 \geq 2(x^r - a)(x - x^r) + (x^r - a)^2. \tag{45}$$

Proof: It is obvious that the quadratic function is convex with respect to x. Recall that the value of the convex function is larger than or equal to that of its first-order Taylor expansion at any point, we can obtain (45). ■

Thus, according to Lemma 2, with given $x^r[n]$ and $y^r[n]$, we have

$$(x[n] - x_e)^2 \geq 2(x^r[n] - x_e)(x[n] - x^r[n]) + (x^r[n] - x_e)^2, \tag{46}$$

$$(y[n] - y_e)^2 \geq 2(y^r[n] - y_e)(y[n] - y^r[n]) + (y^r[n] - y_e)^2. \tag{47}$$

Finally, according to the above transformations, the original optimization subproblem (SP12) can be approximatively transformed into a convex optimization problem as shown in Proposition 2.

Proposition 2: The optimization subproblem (SP12) can be expressed as (48) approximatively, which is convex and its optimal objective value is a lower bound of that of subproblem (SP12) in (17).

$$\max_{\mathbf{x},\mathbf{y},\mathbf{S}} \ \phi_3 \tag{48a}$$

$$s.t. \ \frac{1}{N}\sum_{n=1}^{N} \alpha_{i_3}[n] \left(\check{r}_{u,i_3}[n] - \hat{r}_{u,e}[n]\right) \geq \phi_3, \forall i_3 \in \mathcal{I}_3, \tag{48b}$$

$$\frac{1}{N}\sum_{n=1}^{N} \alpha_{i_l}[n] \left(\check{r}_{u,i_l}[n] - \hat{r}_{u,e}[n] + \check{r}_{ei_l}[n]\right) \geq \eta, l = 1, 2, \tag{48c}$$

$$\frac{1}{N}\sum_{n=1}^{N} \alpha_{i_l}[n]\check{r}_{u,i_l}[n] \geq \beta^{[i_j]}, l = 1, 2, 3, \tag{48d}$$

$$\frac{1}{N}\sum_{n=1}^{N} \alpha_b[n]\check{r}_{u,b}[n] \geq \gamma, \tag{48e}$$

$$x[1] = x[N] = x_0, y[1] = y[N] = y_0, \tag{48f}$$

$$(x[n+1] - x[n])^2 + (y[n+1] - y[n])^2 \leq d_\varsigma^2, \ n = 1, 2, \ldots, N-1, \tag{48g}$$

$$S_{xe}[n] \leq (x^r[n] - x_e)^2 + 2(x^r[n] - x_e)(x[n] - x^r[n]), \forall n, \tag{48h}$$

$$S_{ye}[n] \leq (y^r[n] - y_e)^2 + 2(y^r[n] - y_e)(y[n] - y^r[n]), \forall n. \tag{48i}$$

Proof: Since $\check{r}_{u,k}[n]$ is concave with respect to $x[n]$ and $y[n]$, $k = b, i_1, i_2, i_3$, the constraints in (48c), (48d) and (48e) are convex. The constraint in is convex because $\check{r}_{u,i_3}[n]$ is concave and $\hat{r}_{u,e}[n]$ is convex. In addition, according to the inequalities (46) and (47), the constraints of slack variables can be transformed into linear constrains as (48h) and (48i). Thus, the optimization subproblem (48) is convex. On the other hand, we can conclude that any feasible solution of the subproblem (48) can also make the subproblem (SP12) feasible, but the reverse is not always true. Thus, the optimal objective value of the subproblem (48) is less than or equal to that of the subproblem (SP12), which is a suboptimal solution. ■

Therefore, according to all the above transformations, the optimization problem (48) can be solved efficiently by using standard convex optimization tools such as CVX, since it has been changed into convex.

C. Iterative Algorithm

According to the above two subproblems, we propose an iterative algorithm to solve (SP11) and (48) alternately until convergent, and the suboptimal solutions of (P1) can be obtained. The algorithm is summarized as follows.

Algorithm 1 Iterative algorithm for (P1)

1: Initialize $\mathbf{x}^r$ and $\mathbf{y}^r$. Set $r = 0$.
2: **repeat**
3: Solve the subproblem (SP11) under given $\mathbf{x}^r$ and $\mathbf{y}^r$, and update the solution as $\mathbf{A}^{r+1}$.
4: Solve the subproblem (48) under given $\mathbf{A}^{r+1}$, and update the solution as $\mathbf{x}^{r+1}$ and $\mathbf{y}^{r+1}$.
5: Update $r = r + 1$.
6: **until** The fractional increase of the objective value is below a predefined threshold $\epsilon > 0$.

Since Algorithm 1 only needs to solve a standard linear programming of (16) and a convex optimization problem of (48) in each iteration, it can be solved with polynomial complexity in the worst case [35]. In addition, the convergence of Algorithm 1 is proved in Proposition 3.

Proposition 3: Algorithm 1 can be guaranteed to converge at the suboptimal solutions for the original problem (P1$''$).

Proof: Define

$$R_{s3}(\mathbf{A},\mathbf{x},\mathbf{y}) = \min\left(\frac{1}{N}\sum_{n=1}^{N}\alpha_{i_3}[n]\left(r_{u,i_3}[n]-r_{u,ei_3}[n]\right)\right), \quad \forall i_3 \in \mathcal{I}_3, \tag{49}$$

$$\check{R}_{s3}(\mathbf{A},\mathbf{x},\mathbf{y}) = \min\left(\frac{1}{N}\sum_{n=1}^{N}\alpha_{i_3}[n]\left(\check{r}_{u,i_3}[n]-\hat{r}_{u,e}[n]\right)\right), \quad \forall i_3 \in \mathcal{I}_3. \tag{50}$$

Firstly, in the $(r+1)$th iteration, because the optimal solution $\mathbf{A}^{r+1}$ can be obtained by solving the subproblem (SP11) under given $\mathbf{x}^r$ and $\mathbf{y}^r$, we have

$$R_{s3}(\mathbf{A}^r,\mathbf{x}^r,\mathbf{y}^r) \le R_{s3}(\mathbf{A}^{r+1},\mathbf{x}^r,\mathbf{y}^r). \tag{51}$$

Second, according to the fact that the value of the function is equal to that of it's first-order Taylor expansion at the given local points, we have

$$R_{s3}(\mathbf{A}^{r+1},\mathbf{x}^r,\mathbf{y}^r) = \check{R}_{s3}(\mathbf{A}^{r+1},\mathbf{x}^r,\mathbf{y}^r). \tag{52}$$

Then, since the optimal solution $\mathbf{x}^{r+1}$ and $\mathbf{y}^{r+1}$ are obtained by solving the subproblem (43) under given $\mathbf{A}^{r+1}$, we have

$$\check{R}_{s3}(\mathbf{A}^{r+1},\mathbf{x}^r,\mathbf{y}^r) \le \check{R}_{s3}(\mathbf{A}^{r+1},\mathbf{x}^{r+1},\mathbf{y}^{r+1}). \tag{53}$$

Finally, because the optimal objective value of subproblem (48) is the lower bound of that of the subproblem (SP12), we have

$$\check{R}_{s3}(\mathbf{A}^{r+1},\mathbf{x}^{r+1},\mathbf{y}^{r+1}) \le R_{s3}(\mathbf{A}^{r+1},\mathbf{x}^{r+1},\mathbf{y}^{r+1}). \tag{54}$$

Thus, based on (51)-(54), we can obtain

$$R_{s3}(A^r,\mathbf{x}^r,\mathbf{y}^r) \le R_{s3}(A^{r+1},\mathbf{x}^{r+1},\mathbf{y}^{r+1}). \tag{55}$$

From (55), we can know that the optimal objective value of problem (P1$''$) is non-decreasing and finite over iterations. As a result, the proposed algorithm is guaranteed to converge at the suboptimal solutions for the original problem (P1$''$) [11], [36], [37]. ■

According to the results of Algorithm 1, $\alpha_{i_l}[n], l = 1, 2, 3$, should be changed back into binary. If the optimized values of $\alpha_{i_l}[n]$ can converge to binary, this relaxation does not have any influence on the optimization. Otherwise, we can reconstruct $\alpha_{i_l}[n]$ by further dividing each time slot into $\tau \ge 1$ sub-slots according to [4]. Then, the number of sub-slots assigned to User i_l in the nth time slot can be denoted as $\mathcal{N}_{i_l}[n] = \tau\alpha_{i_l}[n]$. It is obvious that as τ increases, $\mathcal{N}_{i_l}[n]$ will approach an integer.

IV. Security Optimization Without Caching

In the previous sections, we improve the network security by optimizing UAV trajectory and time scheduling with caching. In this section, we consider another scenario where no user is equipped with cache. At this point, any user is easy to be eavesdropped. To guarantee the secure transmission, we maximize the minimum secrecy rate among all users through jointly optimizing UAV trajectory and time scheduling, which can be formulated as

$$\begin{aligned}
(\text{P2}) \max_{\mathbf{A},\mathbf{x},\mathbf{y}} \quad & \phi && (56a)\\
s.t.\ & \bar{R}_s^{[i]} \ge \phi,\ \forall i \in \mathcal{I}_1 \cup \mathcal{I}_2 \cup \mathcal{I}_3 \cup \mathcal{I}_4 && (56b)\\
& R_u \ge \gamma, && (56c)\\
& \alpha_b[m] = 1,\ \forall m = 1, 2, ..., N_1, && (56d)\\
& \alpha_b[n] = 0,\ \forall n = N_1 + 1, ..., N, && (56e)\\
& \alpha_i[n] = \{0, 1\},\ \forall n, \forall i, && (56f)\\
& \alpha_b[n] + \sum_{i=1}^{4}\alpha_i[n] \le 1,\ \forall n, && (56g)\\
& x[1] = x[N] = x_0, y[1] = y[N] = y_0, && (56h)\\
& (x[n+1]-x[n])^2 + (y[n+1]-y[n])^2 \le d_\varsigma^2, \\
& n = 1, 2, \ldots, N-1, && (56i)
\end{aligned}$$

where the constraint (56g) implies that the UAV only communicates with at most one ground node at each time slot. The average secrecy rate of User i in (56b) can expressed as

$$\bar{R}_s^{[i]} = \frac{1}{N}\sum\nolimits_{n=1}^{N}\left[\alpha_i[n]\left(\bar{r}_{u,i}[n]-r_{u,e3}[n]\right)\right]^+, \tag{57}$$

where

$$\bar{r}_{u,i}[n] = \log_2\left(1+\frac{P_2\rho_0}{\sigma^2\left(H^2+(x[n]-x_i)^2+(y[n]-y_i)^2\right)}\right). \tag{58}$$

Similarly, the optimization problem (P2) can be approximatively divided into two convex subproblems: (SP21) for the UAV time scheduling optimization with fixed trajectory and (SP22) for the UAV trajectory optimization with fixed time

scheduling as follows.

$$(\text{SP21}) \max_{\mathbf{A}} \quad \phi \tag{59a}$$

$$s.t. \ \frac{1}{N}\sum_{n=1}^{N}\alpha_i[n]\left(\bar{r}_{u,i}[n]-r_{u,e3}[n]\right)\geq\phi, \ \forall i, \tag{59b}$$

$$\frac{1}{N}\sum_{n=1}^{N}\alpha_b[n]r_{u,b}[n]\geq\gamma, \tag{59c}$$

$$\alpha_b[m]=1, \ \forall m=1,2,...,N_1, \tag{59d}$$

$$\alpha_b[n]=0, \ \forall n=N_1+1,...,N, \tag{59e}$$

$$0\leq\alpha_i[n]\leq 1, \ \forall n,\forall i, \tag{59f}$$

$$\alpha_b[n]+\sum_{i=1}^{4}\alpha_i[n]\leq 1, \ \forall n. \tag{59g}$$

$$(\text{SP22}) \max_{\mathbf{x},\mathbf{y},\mathbf{S}} \quad \phi \tag{60a}$$

$$s.t. \ \frac{1}{N}\sum_{n=1}^{N}\alpha_i[n]\left(\check{\bar{r}}_{u,i}[n]-\hat{r}_{u,e3}[n]\right)\geq\phi,\forall i, \tag{60b}$$

$$\frac{1}{N}\sum_{n=1}^{N}\alpha_b[n]\check{r}_{u,b}[n]\geq\gamma, \tag{60c}$$

$$x[1]=x[N]=x_0, y[1]=y[N]=y_0, \tag{60d}$$

$$(48g),(48h),(48i). \tag{60e}$$

Since the subproblems (SP21) and (SP22) above are both convex, they can be solved efficiently by using standard convex optimization tools. Then, similar iterative algorithm as Algorithm 1 can solve the subproblems (SP21) and (SP22) alternately until convergence. Therefore, we can obtain the optimal solutions of the problem (P2) accordingly.

V. Simulation Results and Discussion

In this section, we provide numerical simulation results to demonstrate the performance of our proposed UAV relaying network for secure transmission. We first take four typical users, i.e., $\mathcal{I}_1=\{1\}$, $\mathcal{I}_2=\{2\}$, $\mathcal{I}_3=\{3\}$, and $\mathcal{I}_4=\{4\}$. Set the horizontal locations of the BS and the users are $\mathbf{w}_b=(-1000\,\text{m},0\,\text{m})$, $\mathbf{w}_1=(500\,\text{m},500\,\text{m})$, $\mathbf{w}_2=(500\,\text{m},-500\,\text{m})$, $\mathbf{w}_3=(1000\,\text{m},0\,\text{m})$, and $\mathbf{w}_4=(0\,\text{m},0\,\text{m})$ respectively. For simplicity, we assume that all the files have the same size equal to 150 Mbits, i.e., $W_i=150$ Mbits, $\forall i$. We also set $\gamma=3$ bit/s/Hz, $\beta=1$ bit/s/Hz and $\eta=0.75$ bit/s/Hz. In addition, we assume that the time allocated for the UAV obtaining files from the BS is half of the total period, i.e. $N_1\varsigma=0.5N\varsigma$. Unless stated, other parameters in the simulations are given in Table I.

In Fig. 2, we show the UAV trajectory for different schemes with $\mathbf{w}_e=(500\,\text{m},0\,\text{m})$. We adopt the elliptical trajectory (Scheme 1) and the linear trajectory (Scheme 2) as benchmarks, while our proposed scheme is named as Scheme 3. In Scheme 1 and Scheme 2, the time scheduling is optimized with given trajectory, T is set to be 200 s, and $N=200$. In Scheme 3, we set $T>\frac{2L}{V_{max}}=80$ s to guarantee the convergence of UAV trajectory. From the results, we can see that the UAV can fly closer to each user to obtain better performance in our proposed scheme, and the performance can be still improved with larger T.

TABLE I
Parameters for the Simulations

UAV flight altitude	$H=100\,\text{m}$ [4], [11]
UAV maximum speed	$V_{\max}=50\,\text{m/s}$ [4], [11]
BS transmit power	$P_1=0.1\,\text{W}$
UAV transmit power	$P_2=0.1\,\text{W}$ [4]
Noise power	$\sigma^2=-110\,\text{dBm}$ [4]
Reference channel power for $d_0=1$ m	$\rho_0=-60\,\text{dB}$ [4]
Power allocation coefficients	$\theta_1=\theta_2=0.5$

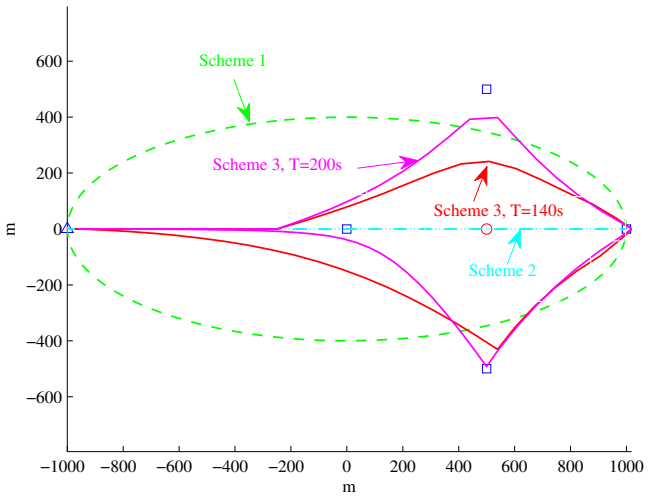

Fig. 2. Comparison of UAV trajectory for different schemes and different T, when $\mathbf{w}_e=(500\,\text{m},0\,\text{m})$.

According to the optimized scheduling and trajectory in Fig. 2, we compare the secrecy rate (SR) of the 2nd user and the 3rd user for different period T and different schemes in Fig. 3 and Fig. 4, when the horizontal location of the eavesdropper is set to $\mathbf{w}_e=(500\,\text{m},0\,\text{m})$ and $\mathbf{w}_e=(700\,\text{m},0\,\text{m})$, respectively. ς=2 s. From the results in Fig. 3, we can see that the secrecy rate of the 3rd user in our proposed scheme can be improved effectively with larger T, due to the optimization of trajectory and scheduling. For the 3rd user in Scheme 1 and Scheme 2, its secrecy rate is much lower than that in our proposed scheme. We can also see that the secrecy rate of the 2rd user is almost the same in these three schemes, and will be nearly unchanged with T. This is because the secrecy rate of the 1st and 2rd user can be mainly guaranteed via caching as we analyzed. In Fig. 4, the eavesdropper is set to $\mathbf{w}_e=(700\,\text{m},0\,\text{m})$, which is farther away from the 1st user and the 2nd user and closer from the 3 user. From the results, we can see that the secrecy rate of the 3rd user in our proposed scheme can be still improved by optimizing the trajectory and scheduling. However, the secrecy rate of the 3rd user in Scheme 1 and Scheme 2 cannot be guaranteed, which is even much lower than the 2rd user.

In Fig. 5, the secrecy rate of our proposed scheme is compared with different number of time slots N_1 allocated for the UAV to obtain files from the BS, when $\mathbf{w}_e=(500\,\text{m},0\,\text{m})$, $T=200$ s, $N=200$. From the results, we can see that the secrecy rate of the 3rd user decreases with N_1, because less

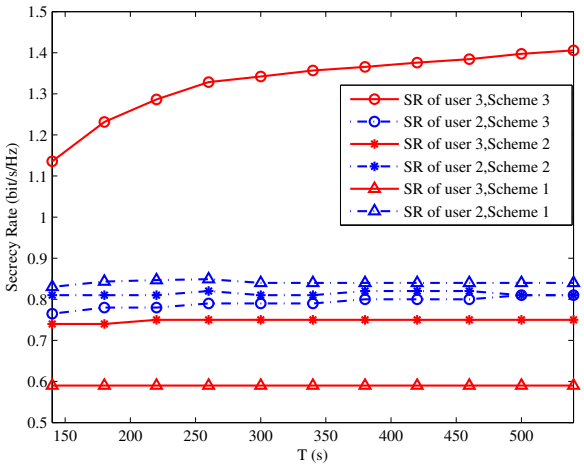

Fig. 3. Secrecy rate comparison of the 2nd user and the 3rd user for different schemes and different T, when the horizontal location of the eavesdropper is $\mathbf{w}_e = (500\,\text{m}, 0\,\text{m})$.

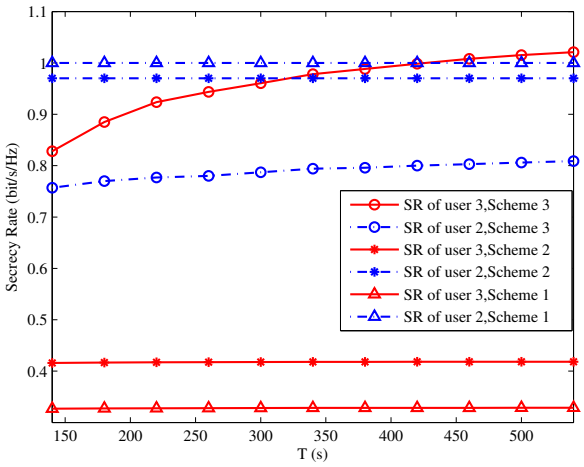

Fig. 4. Secrecy rate comparison of the 2nd user and the 3rd user for different schemes and different T, when the horizontal location of the eavesdropper is $\mathbf{w}_e = (700\,\text{m}, 0\,\text{m})$.

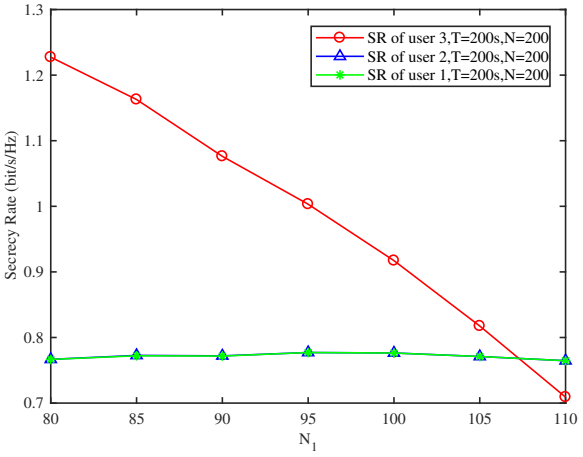

Fig. 5. Secrecy rate comparison of our proposed scheme with different number of time slots N_1 allocated for the UAV to obtain files from the BS, when $\mathbf{w}_e = (500\,\text{m}, 0\,\text{m})$.

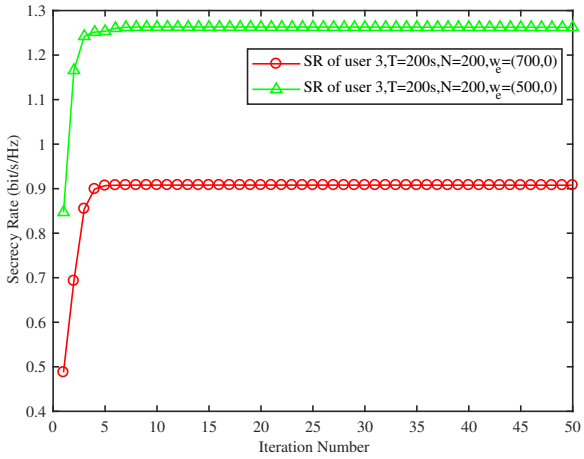

Fig. 6. Secrecy rate convergence of the 3rd user in Algorithm 1, when $T = 200$ s and $N = 200$.

time slots will be allocated to the 3rd user to guarantee its security. For the 1st and 2nd users, the secrecy rate remains almost unchanged with different N_1, due to the fact that their security is mainly guaranteed via caching. On the other hand, we cannot set N_1 too small, otherwise, the constraint (13d) cannot be satisfied. Thus, we can conclude that N_1 should be set as small as possible to achieve better performance, on the condition that the optimization problem can be solved.

The convergence of Algorithm 1 for our proposed scheme is shown in Fig. 6, when $T = 200$ s and $N = 200$. From the results, we can see that the proposed Algorithm 1 can be guaranteed to converge for both $\mathbf{w}_e = (700\,\text{m}, 0\,\text{m})$ and $\mathbf{w}_e = (500\,\text{m}, 0\,\text{m})$ within about 5 iterations, which is consistent with the analysis in Proposition 1. In addition, recall that we only need to solve two convex problems in each iteration, and the computational complexity of Algorithm 1 is appropriate for practical applications.

In the simulations above, we assume that the 4th user can obtain the required file from its local cache directly, the 1st user and the 2nd user receive files cooperatively via caching, and the 3rd user does not cache the required file, which can be defined as Case 1. To analyze the performance of the proposed scheme much more comprehensively, more cases are considered in Fig. 7 and Table II. First, the optimized UAV trajectories are shown in Fig. 7. From the results, we can observe that the UAV flies close to the user without caching within several time slots to transmit the files in all the cases. On the contrary, it is not necessary for the UAV to fly close to the cached-enabled users and stay there to broadcast the files, due to the fact that the secrecy rate of these users can be guaranteed through transmitting the pre-cached files cooperatively to confuse the eavesdropper. Then, the secrecy rate of the users in different cases are presented in Table II, where ★ means that the file required for the user already exists in its local cache and bold data are the secrecy rate of the users without caching in different cases. From the results, we can see that the secrecy rate of the user without caching in Case 3 to Case 6 are higher than that in Case 1 and Case 2. This is because the user without caching in Case 3 to Case

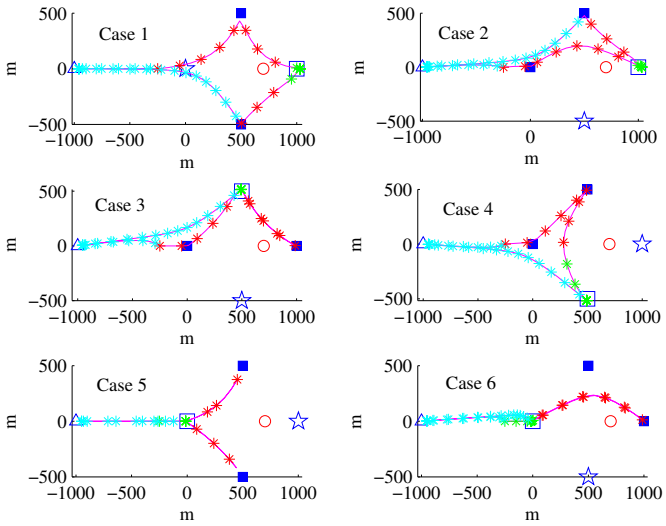

Fig. 7. Optimized trajectories for different cases. The BS is marked by blue '△' and the eavesdropper is marked by red '◯'. The user whose required file already exists in its local cache is marked by blue '☆', the two cooperative caching users are marked by blue ■, and the user without cached file is marked by blue '□'. The trajectory is sampled every 4 s and marked with '∗'. The sampled points marked by cyan '∗' show that the UAV obtains files from the BS. The sampled points marked by red '∗' indicate that the UAV broadcasts files to two cooperative caching users. The sampled points marked by green '∗' mean that the UAV transmits file to the user without caching.

TABLE II
SECRECY RATE FOR THE USERS IN DIFFERENT CASES

SR (bit/s/Hz)	User 1	User 2	User 3	User 4
Case 1	0.7765	0.7764	**0.9078**	★
Case 2	0.8000	★	**0.9994**	0.8000
Case 3	**1.3691**	★	0.7962	0.7962
Case 4	0.8251	**1.4556**	★	0.8251
Case 5	0.8256	0.8256	★	**1.4597**
Case 6	0.7956	★	0.7956	**1.5938**

6 is farther away from the eavesdropper than the user in Case 1 and Case 2.

Furthermore, we consider a more general case with six users, which are randomly distributed. In the simulation, User 1 and User 2 have cached the files that are required for each other, User 3, User 4 and User 5 have no caching capability, and User 6 has already cached its required file, i.e., $\mathcal{I}_1 = \{1\}$, $\mathcal{I}_2 = \{2\}$, $\mathcal{I}_3 = \{3, 4, 5\}$ and $\mathcal{I}_4 = \{6\}$. We aim to maximize the minimum secrecy rate of all the uncached users by jointly optimizing the UAV trajectory and time scheduling, with the secrecy rate of other caching users guaranteed. We set $T = 200$ s, $N = 100$, $N_1 = 40$, $\gamma = 3.5$ bit/s/Hz, $\beta = 0.7$ bit/s/Hz and $\eta = 0.6$ bit/s/Hz. The optimized UAV trajectory is shown in in Fig. 8, and the secrecy rate of the users are presented in Table III. From the results, we can conclude that our proposed scheme can also be utilized in the general case of more users with reliable performance. Specifically, the minimum secrecy rate of all the uncached users can be optimized to be 0.607 bit/s/Hz, with the secrecy rate of cached users higher than $\eta = 0.6$ bit/s/Hz.

Finally, we consider the scenario in which no user has caching ability, and we maximize the minimum secrecy rate

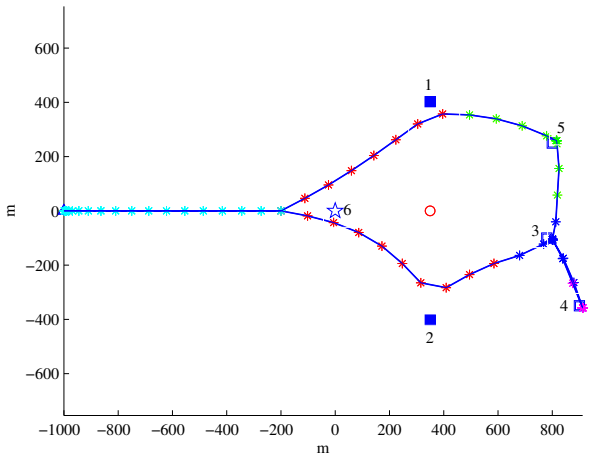

Fig. 8. Optimized UAV trajectory for the case of 6 users. The BS is marked by blue '△' and the eavesdropper is marked by red '◯'. The user with its required file cached is marked by blue '☆', the cooperated caching users are marked by blue '■', and the users without caching are marked by blue '□'. Each trajectory is sampled each 2 s and marked with '∗'. The sampled points marked by cyan '∗' show that the UAV obtains files from the BS. The points marked by red '∗' indicate that the UAV broadcasts files to the cached users. The points marked by blue, mauve and green '∗' show that the UAV transmits files to the uncached users 3, 4, and 5, respectively.

TABLE III
SECRECY RATE OF THE CASE WITH 6 USERS

SR (bit/s/Hz)	User 1	User 2	User 3	User 4	User5
	0.635	0.635	0.607	0.607	0.607

among all users by jointly optimizing the UAV trajectory and time scheduling according to (P2). The optimized UAV trajectories with different locations of the eavesdropper are presented in Fig. 9, with γ=4 bit/s/Hz. For comparison, the optimized UAV trajectories of our proposed scheme with caching are also presented in Fig. 10. From the results, we can see that in the proposed scheme with caching, the UAV can serve the two users with caching on in a much larger range and serve the 3rd user without caching only when it flies above it. This is because the secrecy rate of the two caching users can be mainly guaranteed through transmitting the pre-cached files cooperatively to confuse the eavesdropper. While in benchmark system model without caching, we can see that the UAV will serve a specific user if and only if the distance between the UAV and the user does not exceed the distance between the UAV and the eavesdropper. This is because the instantaneous secrecy rate of all the users in each time slot should be higher than 0; otherwise, the UAV will serve other users with positive secrecy rate to improve the network security. In addition, the secrecy rate of each user in the proposed and benchmark schemes is compared in Table IV when $\mathbf{w}_e = (700\,\mathrm{m}, 0\,\mathrm{m})$. From the results, we can observe that the secrecy rate of each user in the proposed scheme with caching is much higher than that in the benchmark scheme without caching. Thus, we can conclude that cooperative caching can significantly improve the security for the UAV relaying assisted networks.

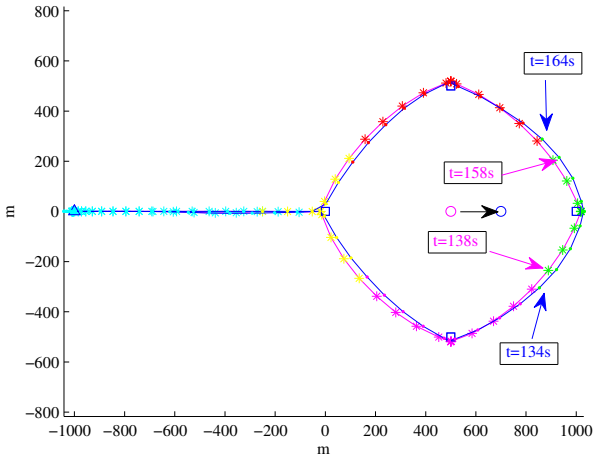

Fig. 9. Optimized trajectory for maximizing the minimum secrecy rate over all users without caching. The BS is marked by blue '△', the users are marked by blue '□' and the eavesdropper is marked by mauve '◯' when $\mathbf{w}_e = (500\,\mathrm{m}, 0\,\mathrm{m})$ or blue '◯' when $\mathbf{w}_e = (700\,\mathrm{m}, 0\,\mathrm{m})$. The mauve curve is optimal UAV trajectory when $\mathbf{w}_e = (500\,\mathrm{m}, 0\,\mathrm{m})$, while the blue curve is optimal UAV trajectory when $\mathbf{w}_e = (700\,\mathrm{m}, 0\,\mathrm{m})$. Each trajectory is sampled every 2 s and marked with '$*$' or '.'. The sampled points marked by cyan '$*$' show that the UAV obtains files from the BS. The sampled points marked by red '$*$', mauve'$*$', green '$*$' and yellow '$*$' indicate that the UAV transmits file to the 1st user, the 2nd user, the 3rd user and the 4th user when $\mathbf{w}_e = (500\,\mathrm{m}, 0\,\mathrm{m})$, respectively. When $\mathbf{w}_e = (700\,\mathrm{m}, 0\,\mathrm{m})$, the marks '$*$' are replaced by '.'.

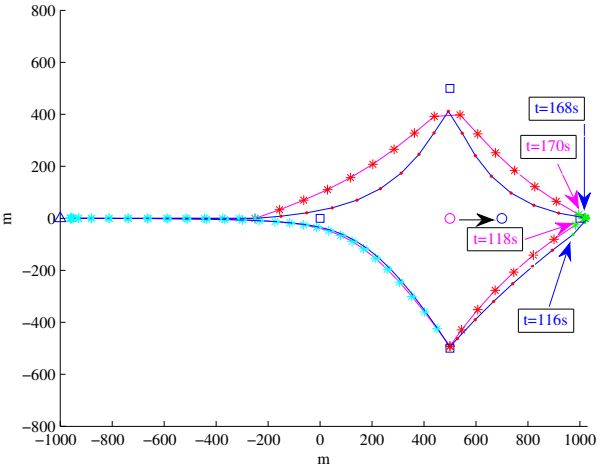

Fig. 10. Optimized trajectory for maximizing the minimum secrecy rate over all users with caching. The markers are similar to those in Fig. 9.

VI. Conclusions

In this paper, the security of UAV-relayed wireless networks with caching has been studied. In our proposed scheme, the UAV first obtains the files from the BS and then transmits them to the users. The users with caching capability can pre-cache some files during off-peak time. When two users have cached the file required by the other, the UAV can broadcast the files to them and disrupt the eavesdropping. For the users without caching, their security can be guaranteed by optimizing the UAV trajectory. Thus, we propose to maximize the minimum secrecy rate of the uncached users via jointly optimizing the UAV trajectory and time scheduling, with the performance requirement of caching users satisfied. The problem is non-convex, which is divided into two subproblems, and an iterative algorithm is proposed to solve them alternately. In addition, we also consider the scenario in which no user is equipped with cache as a benchmark. Simulation results are finally presented to show the effectiveness and efficiency of the secure transmission in proposed UAV relaying systems with local caching.

TABLE IV
Secrecy Rate of the Proposed and Benchmark Schemes

SR (bit/s/Hz)	User 1	User 2	User 3	User 4
Proposed Scheme	0.7765	0.7764	0.9078	★
Benchmark Scheme	0.3908	0.3908	0.3908	0.3908

References

[1] Y. Zeng, R. Zhang, and T. J. Lim, "Wireless communications with unmanned aerial vehicles: opportunities and challenges," *IEEE Commun. Mag.*, vol. 54, no. 5, pp. 36–42, May 2016.

[2] A. A. Khuwaja, Y. Chen, N. Zhao, M.-S. Alouini, and P. Dobbins, "A survey of channel modeling for UAV communications," *IEEE Commun. Surv. Tuts.*, vol. 20, no. 4, pp. 2804–2821, 4th Quart. 2018.

[3] J. Lyu, Y. Zeng, R. Zhang, and T. J. Lim, "Placement optimization of UAV-mounted mobile base stations," *IEEE Commun.Lett.*, vol. 21, no. 3, pp. 604–607, Mar. 2017.

[4] Q. Wu, Y. Zeng, and R. Zhang, "Joint trajectory and communication design for multi-UAV enabled wireless networks," *IEEE Trans. Wireless Commun.*, vol. 17, no. 3, pp. 2109–2121, Mar. 2018.

[5] X. Liu, Z. Li, N. Zhao, W. Meng, G. Gui, Y. Chen, and F. Adachi, "Transceiver design and multi-hop D2D for UAV IoT coverage in disasters," *IEEE Internet Things J.*, Online, DOI: 10.1109/JIOT.2018.2877504.

[6] Y. Zeng, X. Xu, and R. Zhang, "Trajectory design for completion time minimization in UAV-enabled multicasting," *IEEE Trans. Wireless Commun.*, vol. 17, no. 4, pp. 2233–2246, Apr. 2018.

[7] N. Zhao, F. Cheng, F. R. Yu, J. Tang, Y. Chen, G. Gui, and H. Sari, "Caching UAV assisted secure transmission in hyper-dense networks based on interference alignment," *IEEE Trans. Commun.*, vol. 66, no. 5, pp. 2281–2294, May 2018.

[8] J. Lyu, Y. Zeng, and R. Zhang, "UAV-aided offloading for cellular hotspot," *IEEE Trans. Wireless Commun.*, vol. 17, no. 6, pp. 3988–4001, Jun. 2018.

[9] F. Cheng, S. Zhang, Z. Li, Y. Chen, N. Zhao, F. R. Yu, and V. C. M. Leung, "UAV trajectory optimization for data offloading at the edge of multiple cells," *IEEE Trans. Veh. Technol.*, vol. 67, no. 7, pp. 6732–6736, Jul. 2018.

[10] D. Yang, Q. Wu, Y. Zeng, and R. Zhang, "Energy tradeoff in ground-to-UAV communication via trajectory design," *IEEE Trans. Veh. Technol.*, vol. 67, no. 7, pp. 6721–6726, Jul. 2018.

[11] Y. Zeng, R. Zhang, and T. J. Lim, "Throughput maximization for UAV-enabled mobile relaying systems," *IEEE Trans.Commun.*, vol. 64, no. 12, pp. 4983–4996, Dec. 2016.

[12] S. Zeng, K. H. Zhang, and L. Song, "Uav relaying: Power allocation and trajectory optimization using decode-and-forward protocol,," in *Proc. IEEE ICC'18*, pp. 1–6, Kansas City, MO, USA, May. 2018.

[13] S. Zhang, H. Zhang, Q. He, K. Bian, and L. Song, "Joint trajectory and power optimization for UAV relay networks," *IEEE Commun. Lett.*, vol. 22, no. 1, pp. 161–164, Jan. 2018.

[14] J. Li and Y. Han, "Optimal resource allocation for packet delay minimization in multi-layer UAV networks," *IEEE Commun.Lett.*, vol. 21, no. 3, pp. 580–583, Mar. 2017.

[15] M. Chen, M. Mozaffari, W. Saad, C. Yin, M. Debbah, and C. S. Hong, "Caching in the sky: Proactive deployment of cache-enabled unmanned aerial vehicles for optimized quality-of-experience," *IEEE J. Sel. Areas. Commun.*, vol. 35, no. 5, pp. 1046–1061, May 2017.

[16] M. Chen, W. Saad, and C. Yin, "Liquid state machine learning for resource and cache management in LTE-U unmanned aerial vehicle (UAV) networks." Available: https://arxiv.org/abs/1801.09339, Jan 2018.

[17] X. Xu, Y. Zeng, Y. L. Guan, and R. Zhang, "Overcoming endurance issue: UAV-enabled communications with proactive caching," *IEEE J. Sel. Areas on Commmun.*, vol. 36, no. 6, pp. 1231–1244, Jun. 2018.

[18] Y. Zou, J. Zhu, X. Wang, and L. Hanzo, "A survey on wireless security: Technical challenges, recent advances, and future trends," *Proc. IEEE*, vol. 104, no. 9, pp. 1727–1765, Sept. 2016.

[19] N. Yang, L. Wang, G. Geraci, M. Elkashlan, J. Yuan, and M. D. Renzo, "Safeguarding 5G wireless communication networks using physical layer security," *IEEE Commun. Mag.*, vol. 53, no. 4, pp. 20–27, Apr. 2015.

[20] P. K. Gopala, L. Lai, and H. E. Gamal, "On the secrecy capacity of fading channels," *IEEE Trans. Inf. Theory*, vol. 54, no. 10, pp. 4687–4698, Oct. 2008.

[21] F. Zhu, F. Gao, M. Yao, and H. Zou, "Joint information- and jamming-beamforming for physical layer security with full duplex base station," *IEEE Trans. Signal Process.*, vol. 62, no. 24, pp. 6391–6401, Dec. 2014.

[22] H. M. Wang and X. G. Xia, "Enhancing wireless secrecy via cooperation: signal design and optimization," *IEEE Commun. Mag.*, vol. 53, no. 12, pp. 47–53, Dec. 2015.

[23] L. Fan, R. Zhao, F. K. Gong, N. Yang, and G. K. Karagiannidis, "Secure multiple amplify-and-forward relaying over correlated fading channels," *IEEE Trans. Commun.*, vol. 65, no. 7, pp. 2811–2820, Jul. 2017.

[24] N. Zhao, F. R. Yu, M. Li, Q. Yan, and V. C. M. Leung, "Physical layer security issues in interference-alignment-based wireless networks," *IEEE Commun. Mag.*, vol. 54, no. 8, pp. 162–168, Aug 2016.

[25] Y. Cao, N. Zhao, F. R. Yu, M. Jin, Y. Chen, J. Tang, and V. C. M. Leung, "Optimization or alignment: Secure primary transmission assisted by secondary networks," *IEEE J. Sel. Areas Commun.*, vol. 36, no. 4, pp. 905–917, Apr. 2018.

[26] F. Zhou, Z. Chu, H. Sun, R. Q. Hu, and L. Hanzo, "Artificial noise aided secure cognitive beamforming for cooperative MISO-NOMA using SWIPT," *IEEE J. Sel. Areas Commun.*, vol. 36, no. 4, pp. 918–931, Apr. 2018.

[27] F. Shu, L. Xu, J. Wang, W. Zhu, and X. Zhou, "Artificial-noise-aided secure multicast precoding for directional modulation systems," *IEEE Trans. Veh. Technol.*, vol. 67, no. 7, pp. 6658–6662, Jul. 2018.

[28] U. Challita, A. Ferdowsi, M. Chen, and W. Saad, "Machine learning for wireless connectivity and security of cellular-connected UAVs," *IEEE Wireless Commun.*, to appear.

[29] Y. Cai, F. Cui, Q. Shi, M. Zhao, and G. Y. Li, "Dual-UAV-enabled secure communications: Joint trajectory design and user scheduling," *IEEE J. Sel. Areas Commun.*, vol. 36, no. 9, pp. 1972–1985, Sept. 2018.

[30] W. Zhao, Z. Chen, K. Li, B. Xia, and P. Chen, "Artificial interference aided physical layer security in cache-enabled heterogeneous networks," in *Proc. IEEE SPAWC'18*, pp. 1–6, Kalamata, Greece, Jun. 2018.

[31] Q. Wang, Z. Chen, W. Mei, and J. Fang, "Improving physical layer security using UAV-enabled mobile relaying," *IEEE Wireless Commun.Lett.*, vol. 6, no. 3, pp. 310–313, Jun. 2017.

[32] G. Zhang, Q. Wu, M. Cui, and R. Zhang, "Securing UAV communications via trajectory optimization," in *Proc. IEEE GLOBECOM'17*, pp. 1–6, Singapore, Dec. 2017.

[33] M. Caris, S. Stanko, M. Malanowski, P. Samczyski, K. Kulpa, A. Leuther, and A. Tessmann, "mm-wave SAR demonstrator as a test bed for advanced solutions in microwave imaging," *IEEE Aerosp. Electron. Syst. Mag.*, vol. 29, no. 7, pp. 8–15, Jul. 2014.

[34] Z. Ding, X. Lei, G. K. Karagiannidis, R. Schober, J. Yuan, and V. K. Bhargava, "A survey on non-orthogonal multiple access for 5G networks: Research challenges and future trends," *IEEE J. Sel. Areas Commun.*, vol. 35, no. 10, pp. 2181–2195, Oct. 2017.

[35] S. Boyd and L. Vandenberghe, *Convex Optimization*. Cambridge University Press, 2004.

[36] M. F. Hanif, Z. Ding, T. Ratnarajah, and G. K. Karagiannidis, "A minorization-maximization method for optimizing sum rate in the downlink of non-orthogonal mul-tiple access systems," *IEEE Trans. Signal Process.*, vol. 64, no. 1, pp. 76–88, Jan. 2016.

[37] M. Hong, M. Razaviyayn, Z.-Q. Luo, and J.-S. Pang, "A unified algorithmic framework for block-structured optimization involving big data: With applications in machine learning and signal processing," *IEEE Signal Process. Mag.*, vol. 33, no. 1, pp. 57–77, Jan. 2016.

Fen Cheng received the B.S. degree in 2017 from Dalian University of Technology, Dalian, China. She is currently working toward the graduate degree in the School of Information and Communication Engineering, Dalian University of Technology, Dalian, China.

Her current research interests include UAV communications, interference alignment, cache-aided networks, physical layer security, and resource allocation.

Guan Gui (M'11-SM'17) received the Dr. Eng degree in Information and Communication Engineering from University of Electronic Science and Technology of China (UESTC), Chengdu, China, in 2012. From October 2009 to March 2012, with the financial supported from the China scholarship council (CSC) and the global center of education (ECOE) of Tohoku University, he joined the wireless signal processing and network laboratory (Prof. Fumiyuki Adachi laboratory), Department of Communications Engineering, Graduate School of Engineering, Tohoku University as for research assistant as well as postdoctoral research fellow, respectively. From September 2012 to March 2014, he was supported by Japan society for the promotion of science (JSPS) fellowship as postdoctoral research fellow at same laboratory. From April 2014 to October 2015, he was an Assistant Professor in Department of Electronics and Information System, Akita Prefectural University. Since November 2015, he has been a professor with Nanjing University of Posts and Telecommunications (NUPT), Nanjing, China. He is currently engaged in research of deep learning, compressive sensing and advanced wireless techniques. He is a senior member of Institute of Electrical and Electronics Engineers (IEEE). Dr. Gui has been Editor for Security and Communication Networks (2012–2016), editor of IEEE Transactions on Vehicular Technology (2017–) and KSII Transactions on Internet and Information System (2017–). He received several best paper awards such as CSPS2018, ICNC2018, ICC2017, ICC2014 and VTC2014-Spring. He was also selected as for Jiangsu Special Appointed Professor, Jiangsu High-level Innovation and Entrepreneurial Talent and Nanjing Youth Award.

Nan Zhao (S'08-M'11-SM'16) is currently an Associate Professor at Dalian University of Technology, China. He received the Ph.D. degree in information and communication engineering in 2011, from Harbin Institute of Technology, Harbin, China.

Dr. Zhao is serving or served on the editorial boards of 7 SCI-indexed journals, including IEEE Transactions on Green Communications and Networking. He won the best paper awards in IEEE VTC 2017 Spring, MLICOM 2017, ICNC 2018, WCSP 2018 and CSPS 2018. He also received the IEEE Communications Society Asia Pacific Board Outstanding Young Researcher Award in 2018.

Yunfei Chen (S'02-M'06-SM'10) received his B.E. and M.E. degrees in electronics engineering from Shanghai Jiaotong University, Shanghai, P.R.China, in 1998 and 2001, respectively. He received his Ph.D. degree from the University of Alberta in 2006. He is currently working as an Associate Professor at the University of Warwick, U.K. His research interests include wireless communications, cognitive radios, wireless relaying and energy harvesting.

Jie Tang (S'10-M'13-SM'18) received the B.Eng. degree in Information Engineering from the South China University of Technology, Guangzhou, China, in 2008, the M.Sc. degree (with Distinction) in Communication Systems and Signal Processing from the University of Bristol, UK, in 2009, and the Ph.D. degree from Loughborough University, Leicestershire, UK, in 2012. He is currently an associate professor in the School of Electronic and Information Engineering, South China University of Technology, China. He previously held Postdoctoral research positions at the School of Electrical and Electronic Engineering, University of Manchester, UK.

His research interests include green communications, NOMA, 5G networks, SWIPT, heterogeneous networks, cognitive radio and D2D communications. He is currently serving as an Editor for IEEE Access, EURASIP Journal on Wireless Communications and Networking, Physical Communications and Ad Hoc & Sensor Wireless Networks. He also served as a track co-chair for IEEE Vehicular Technology Conference (VTC) Spring 2018. He is a co-recipient of the 2018 IEEE ICNC Best Paper Award.

Hikmet Sari (F'95) is currently Professor of Nanjing University of Posts and Telecommunications (NUPT), and also Chief Scientist of Sequans Communications, a leading developer and supplier of LTE chipset solutions. He received his Engineering Degree and Ph.D. from the ENST, Paris, France, and the post-doctoral Habilitation degree from the University of Paris-Sud, Orsay. Prior to his current positions, he held various research and management positions in industry including Philips Research Laboratories, SAT, Alcatel, Pacific Broadband Communications, and Juniper Networks. His distinctions include the *IEEE Fellow Grade* (1995), the *Andre Blondel Medal* (also in 1995), the *Edwin H. Armstrong Achievement Award* in 2003, the *Harold Sobol Award* in 2012, as well as election to *Academia Europaea* (the Academy of Europe) and to the *Science Academy of Turkey* in 2012.

Prof. Sari has served as an Editor of the IEEE Transactions on Communications (1987-1981), a Guest Editor of the European Transactions on Telecommunications (1993) and of the IEEE JSAC (1999), and an Associate Editor of the IEEE Communications Letters (1999-2002). He served as a Distinguished Lecturer of the IEEE Communications Society in 2001-2006, as a member of the IEEE Fellow Evaluation Committee in 2002-2007, and as a member of the Awards Committee in 2005-2007.

Prof. Sari was Chair of the Communication Theory Symposium of ICC 2002 (New York), Technical Program Chair of ICC 2004 (Paris), Vice General Chair of ICC 2006 (Istanbul), General Chair of PIMRC 2010 (Istanbul), General Chair of WCNC 2012 (Paris), Executive Chair of WCNC 2014 (Istanbul), General Chair of ICUWB 2014 (Paris), General Co-Chair of IEEE BlackSeaCom 2015 (Constanta, Romania), Technical Program Chair of EuCNC 2015 (Paris), and Executive Co-Chair of ICC 2016 (Kuala Lumpur). He also chaired the Globecom and ICC Technical Content (GITC) Committee during the period of 2010 C 2011, and he was Vice President for Conferences of the IEEE Communications Society during 2014 C 2015. Currently, he is serving as General Co-Chair of ATC 2016 (Hanoi, Vietnam), Executive Chair of ICC 2017 (Paris), and General Chair of PIMRC 2019 (Istanbul).